IEEE Access
Multidisciplinary | Rapid Review | Open Access Journal

Received 27 May 2022, accepted 14 June 2022, date of publication 21 June 2022, date of current version 27 July 2022.

Digital Object Identifier 10.1109/ACCESS.2022.3185133

Solving Perturbed Time-Varying Linear Equation and Inequality Problem With Adaptive Enhanced and Noise Suppressing Zeroing Neural Network

CHAOMIN WU, ZIFAN HUANG, JIAHAO WU, AND CONG LIN
School of Electronics and Information Engineering, Guangdong Ocean University, Zhanjiang 524088, China
Corresponding author: Cong Lin (lincong@hainanu.edu.cn)

This work was supported by the Guangdong Basic and Applied Basic Research Foundation under Grant 2021A1515011847.

ABSTRACT Solving time-varying linear equation and inequality (TVLEI) problem has attracted extensive attention in numerous scientific and engineered fields. In this article, it is basically considered that the commonly used dynamics neural network in the virtual environment is inevitably interfered with by the variable measurement noises while dealing with the TVLEI problem. An adaptive enhanced and noise-suppressing zeroing neural network (AENSZNN) model is proposed as an improved algorithm for solving the TVLEI problem. An adaptive scale factor based on the residual error norm is designed to make the proposed AENSZNN model converge to the theoretical solution faster. Furthermore, the momentum enhancement terms added to the model enables the AENSZNN model to effectively solve the TVLEI problem in real-time under the obstruction of different measurement noises. Besides, theoretical results and numerical experiments indicate that the AENSZNN model has advantages in convergence accuracy and robustness to noises compared with the existing algorithms. Note that, the proposed AENSZNN model is successfully exploited for the estimation of mobile object localization.

INDEX TERMS Time-varying linear equation and inequality, noises perturbance, zeroing neural network (ZNN), adaption factor, dynamic positioning.

I. INTRODUCTION

The problem of linear equation and inequality (LEI) generally exists in many fields of science and industry, such as control system [1], stability analysis [2], [3], data handling [4], information retrieval [5], etc. Many engineering and theoretical problems can be simplified as the inherent LEI system. For example, the robot control is modeled by a system of linear equations [6], [7]. In the redundancy robotic manipulators solution, the avoidance characteristics of joint physical constraints corresponds to a linear inequality system [8], [9]. By combining and solving the relevant combined linear equation and inequality system, robots can be successfully controlled without joint physical constraints or environmental obstacles [10]. The LEI problem can be described as the situation that if and only if the solution of $C\vec{x} = \vec{b}$ and the solution of $D\vec{x} \leq \vec{d}$ exist at the same time and the intersection of their solutions is non-empty. Solving such a LEI problem is essentially finding simultaneous solutions that satisfy equation and inequality. Obviously, the LEI problem has a great importance in the variant application, it becomes necessary and meaningful to develop an effective unified solution scheme [11]–[13]. Currently, a lot of studies have been proposed which aim at solving the LEI problem. In paper [14], Gol *et al*. study regularization and find the normal solutions of the linear equations and inequalities systems. Moreover, Li *et al*. analyze and study interval linear equations and inequalities, and demonstrate the feasibility and solvability of the problem in [15]. Besides, Zhou [16] construct an optimal control method for Lyapunov inequality for linear elliptic equation. In paper [17], two kinds of discrete-time neural networks with fast convergence speed are proposed to solve the LEI problem by using the scaling techniques. Furthermore, Liang and Tso [18] utilize the discrete-time zeroing neural network to solve the LEI problem and give the corresponding improved upper limit of the step size parameters. However, it is worth noting that the abovementioned methods are essentially presented to solve the time-invariant LEI problem, which leads to falling into low solution accuracy problem or even system collapse due to the lagging error.

In [19], a special kind of recurrent neural network termed zeroing neural network (ZNN) model is presented as an

The associate editor coordinating the review of this manuscript and approving it for publication was Hongwei Du.

effective scheme to solve varieties of time-varying problems. By making full use of the time derivative information of time-varying parameters, the theoretical solution to the time-varying problems is tracked by the evolution formula. Taking advantage of the method of ZNN [20]–[22], the objective of effectively solving time-varying problems is achieved. Specifically, Xu *et al*. [23] furnish a ZNN model for ensuring the solution of the TVLEI problem, which takes full advantage of the ZNN model as well as the time-derivative information about the time-varying coefficients involved in the time-varying problems. Due to the sensitivity of the model to noises. Specifically, noises will lead to performance degradation, or even lead to the solving system collapse [24]. In view of the lack of convergence speed and poor anti-noise performance of ZNN models, many studies have presented [25], [26]. In [27], a dynamics zeroing neural network with intrinsic noises tolerance aims to suppress additive noises by adding an integral term so that it can converge globally to the theoretical solution precisely. Besides, Xiao *et al*. [28] present a unified ZNN, which simultaneously has both remarkable finite time convergence performance and inherent noises tolerance. In [29], a unified predefined-time convergent and robust ZNN model is put forward to obtain an exact solution in a specified finite time and accuracy can not be affected in the face of high amplitude perturbations. Moreover, by using special activation functions including the well-known sign-bi-power function in ZNN, Xiao *et al*. [30] recommend a finite-time Zhang neural network to make the convergence performance have a remarkable improvement. Despite the design and analysis of the accelerated ZNN models to find the optimum solution having acquired some achievements, the current research has not solved the existing problems. For instance, the learning speed of the model needs to be repeatedly and carefully adjusted. At this time, the model cannot make full use of the residual information in the solution system, which eventually leads to truncation errors or even crash the solution system.

Therefore, this paper proposes an adaptive enhanced and noise-suppressing zeroing neural network (AENSZNN) model which can get the utmost out of the residual error information and momentum information of the solution system. By combining the residual error and the adaption scale factor, the AENSZNN model achieves a faster convergence rate and higher robustness than the previously proposed solution system. That is, this model can not only maintain high robustness under the various measurement noises disturbance but also speed up the convergence of the solving system. A good deal of various algorithms and neural network models have been put forward and applied in solving the TVLEI problem, the specific performance comparison results among them are exhibited in Table 1.

The remainder of this paper is segmented into the following five parts. Section II introduces the preliminary knowledge of the solution of the TVLEI problem. Further, the detailed description of the norm-based adaption factor design method and the AENSZNN model construction method to solve the TVLEI problem is settled in Section III. Next, Section IV strictly analyzes the global convergence and robustness of the AENSZNN model. Besides, an illustrative simulation example 1 (V-A) and the dynamic positioning simulative experiments based on the angle of arrival (AOA) positioning algorithm are provided to verify the effectiveness and superiority of the proposed AENSZNN model in Section V. Finally, Section VI concludes this article with concluding remarks. The main contributions of this paper are as follows:

- As far as we know, this paper is the first work to investigate the time-varying linear equation system based on the norm-based adaption scale factor design framework at present. Furthermore, the proposed model achieves a better performance in convergence speed of the solving system and anti-noise ability over the state-of-the-art methods.
- This paper proposes a new AENSZNN model based on a novel design formula for a real-time-varying linear equation under various noises environment. It is worth mentioning that there is currently no real-time-varying matrix inversion neural network model with noises suppression capability.
- Qualitative and quantitative experiments are designed and executed. The results show that the proposed AENSZNN model is superior to the most advanced neural network methods in terms of accuracy and convergence speed, and can generate noise-suppressing results against various measurement noises.
- Compared with the operational schemes, the AENSZNN model has achieved remarkable advantages in both aspects of robust performance and convergence speed in the actual two-dimensional dynamic positioning application based on the AOA algorithm.

II. PROBLEM FOURMULATION AND PRELIMINARIES

The specific representation of the TVLEI problem can be depicted as

$$\begin{cases} C(t)\vec{x}(t) = \vec{b}(t), \\ D(t)\vec{x}(t) \leq \vec{d}(t), \end{cases} \tag{1}$$

where the time-varying matrices $C(t) \in \mathbb{R}^{m\times n}$ and $D(t) \in \mathbb{R}^{p\times n}$, the time-varying smooth vectors $\vec{b}(t) \in \mathbb{R}^m$, $\vec{d}(t) \in \mathbb{R}^p$, and the vector $\vec{x}(t) \in \mathbb{R}^n$ denotes the theoretical solution of the TVLEI problem (1) which needs to be solved. A nonnegative relaxation variable $\vec{\Lambda}^{\cdot 2}(t) \in \mathbb{R}^p$ is imported to further solving the TVLEI problem (1) [31]:

$$\begin{cases} C(t)\vec{x}(t) = \vec{b}(t), \\ D(t)\vec{x}(t) + \vec{\Lambda}^{\cdot 2}(t) = \vec{d}(t), \end{cases} \tag{2}$$

where superscript $^{\cdot 2}$ denotes the square of each element of $\vec{\Lambda}^{\cdot 2}(t) \in \mathbb{R}^p$. When solving the equation (2) in this paper, $\vec{\Lambda}^{\cdot 2}(t) \in \mathbb{R}^p$ is also an unknown vector to be obtained, by defining the diagonal matrix $H(t) = \mathrm{diag}\{y_1(t), \ldots, y_p(t)\} \in \mathbb{R}^{p\times p}$, $\vec{\Lambda}^{\cdot 2}(\mathrm{t})$ is adapted as

TABLE 1. Comparsions of the results on solving the TVLEI problem (1) by using different itreated algorithms or neural network models.

Model	Derivative Information Involved	Designed for Time Depend--ent Problem	Applied Adaption Parameter	Anti Perturbations	MSSRE under Different Noises Conditions			
					Noises Free	Constant Noises	Random Noises	Linear Noises
Algorithm in [16]	No	No	No	No	NA*	NA*	NA*	NA*
Recurrent neural network in [17]	No	No	No	No	Negligible	Bounded	Bounded	$+\infty^{\ddagger}$
OZNN model in [23]	Yes	Yes	No	No	Negligible	Bounded	Bounded	$+\infty^{\ddagger}$
The proposed AENSZNN (11)	Yes	Yes	Yes	Yes	Negligible	Negligible	BS†	BS†

⋆Note that the recurrent neural network in [17] is constructed to solve the static LEI problem.
⋆NA means that the item cannot be obtained from the algorithm in the corresponding papers.
†BS denotes that the MSSRE of the corresponding situation is bounded tightly.
$^{\ddagger}+\infty$ denotes the positive infinity.

TABLE 2. The definition of notation.

Mathematics Symbol	Actual significance
$C(t) \in \mathbb{R}^{m\times n}$, $D(t) \in \mathbb{R}^{p\times n}$	the time-varying matrices
$\vec{x}(t) \in \mathbb{R}^{n}$	the vector which denotes the theoretical solution of the TVLEI problem
$\vec{b}(t) \in \mathbb{R}^{m}$, $\vec{d}(t) \in \mathbb{R}^{p}$	the time-varying smooth vectors
$\vec{\Lambda}^{\cdot 2} = H(t)\vec{\Lambda}(t)$	an unknown vector need to be obtained
$W(t)$	the time-varying matrix
$H(t) = \mathrm{diag}\{y_1(t), \ldots, y_p(t)\} \in \mathbb{R}^{p\times p}$	the diagonal matrix
$\vec{y}(t) = [\vec{x}^{\mathrm{T}}(t), \vec{\Lambda}^{\mathrm{T}}(t)]^{\mathrm{T}} \in \mathbb{R}^{n+p}$	the augmented vector
$\vec{\delta}(t) = W(t)\vec{y}(t) - \vec{u}(t)$	the error function
$\vec{\Phi}(t) = \vec{\Phi} \in \mathbb{R}^{m+p}$	the constant noises
$\vec{\Phi}(t) = \Phi t \in \mathbb{R}^{m+p}$	linear time-varying noises
$\vec{\Phi}(t) = \vec{v}(t) \in \mathbb{R}^{m+p}$	the bounded random noises
$G(\cdot) \in \mathbb{R}^{n\times n} \to \mathbb{R}$	the adaptive scale factor and the parameter
$\sup(\cdot)$	the upper bound of the parameter

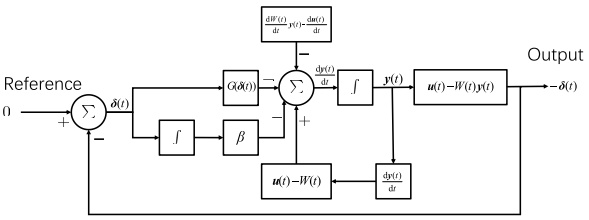

FIGURE 1. From the perspective of the feedback control system, the AENSZNN model (11) for solving the TVLEI problem (1). The structure diagram with the AENSZNN model (11) as the controller.

$\vec{\Lambda}^{\cdot 2} = H(t)\vec{\Lambda}(t)$. Finally, the TVLEI problem (1) is transformed as below:

$$W(t)\vec{y}(t) = \vec{u}(t), \tag{3}$$

where the matrix $W(t) \in \mathbb{R}^{(m+p)\times(n+p)}$ and vector $\vec{u}(t) \in \mathbb{R}^{(m+p)}$ are arranged as

$$W(t) = \begin{bmatrix} C(t) & \vec{0} \\ D(t) & H(t) \end{bmatrix}, \quad \vec{u}(t) = \begin{bmatrix} \vec{b}(t) \\ \vec{d}(t) \end{bmatrix}, \tag{4}$$

the augmented vector $\vec{y}(t) = [\vec{x}^{\mathrm{T}}(t), \vec{\Lambda}^{\mathrm{T}}(t)]^{\mathrm{T}} \in \mathbb{R}^{n+p}$, with the superscript $^{\mathrm{T}}$ denotes the transpose of a matrix or a vector.

III. AN ADAPTIVE ENHANCED AND NOISE SUPPRESSING ZNN MODEL

According to the equation (3) mentioned in Section Π, the corresponding error function is constructed as

$$\vec{\delta}(t) = W(t)\vec{y}(t) - \vec{u}(t). \tag{5}$$

Based on the following OZNN model construction framework to make every element of $\vec{\delta}(t)$ converge to zero, the following equation can be obtained:

$$\dot{\vec{\delta}}(t) = -\gamma\eta(\vec{\delta}(t)), \tag{6}$$

where $\gamma > 0 \in \mathbb{R}$ denotes the scale coefficient and $\eta(\cdot) : \mathbb{R}^{n\times n}$ represents the activation function. Thus, applying the OZNN model to solve the TVLEI problem (1) can be derived as

$$W(t)\dot{\vec{y}}(t) = -\dot{W}(t)\vec{y}(t) - \gamma(W(t)\vec{y}(t) - \vec{u}(t)) + \dot{\vec{u}}(t). \tag{7}$$

However, there will inevitably exist noises interference to the system in practical applications. Concretely speaking, parameter errors, calculation errors, external interference, and modeling errors can all be regarded as noises. Even the rounding error and truncation error in the numerical calculation can be also regarded as noises. Thus, to solve the TVLEI problem (1) in the case of online noises interference, the AENSZNN model is proposed and its evolution formula can be derived as follows:

$$\dot{\vec{\delta}}(t) = -G(\vec{\delta}(t))\vec{\delta}(t) - \beta\int_0^t \vec{\delta}(\tau)\mathrm{d}\tau, \tag{8}$$

where the $G(\cdot) > 0 : \mathbb{R}^{n\times n} \to \mathbb{R}$ represents the adaptive scale factor and the parameter $\beta > 0$. There are several schemes that can be applied to construct the $G(\cdot)$:

- Exponential adaption scale factor scheme:

$$G(\vec{\delta}(t)) = ||\vec{\delta}(t)||_2^{\sigma} + \varphi, \tag{9}$$

  where the parameters $\sigma > 0$ and $\varphi > 1$.
- Power adaption scale factor scheme:

$$G(\vec{\delta}(t)) = \omega^{||\vec{\delta}(t)||_2} + ||(\vec{\delta}(t)||_2, \tag{10}$$

  where the parameter $\omega > 0$.

Through combining the equation (8) and the equation (3), we can obtained:

$$W(t)\dot{\vec{y}}(t) = -G(\vec{\delta}(t))(W(t)\vec{y}(t) - \vec{u}(t)) - \dot{W}(t)\vec{y}(t) + \dot{\vec{u}}(t) - \beta\int_0^t (W(\tau)\vec{y}(\tau) - \vec{u}(\tau))\mathrm{d}\tau. \tag{11}$$

By observing the structure diagram of the AENSZNN model (11) in Fig. 1, we can view the AENSZNN model (11) as a broadly proportional-integral-derivative (PID) controller, which is differential, proportional, and integral control input section respectively as $-\dot{W}(t)\vec{y}(t) + \dot{\vec{u}}(t)$, $-G(\vec{\delta}(t))(W(t)\vec{y}(t) - \vec{u}(t))$, $-\beta\int_0^t(W(\tau)\vec{y}(\tau) - \vec{u}(\tau))\mathrm{d}\tau$. The global convergence performance of the proposed AENSZNN model (11) is a significant criterion. To further

analyze the convergence performance of the AENSZNN model (11) in the case of noises-free. The following theorem is given:

Theorem 1: Given an any solvable TVLEI problem (1), the solution obtained by the AENSZNN model (11) always globally converges to the exact solution. That is to say, the residual error $||\vec{\delta}(t)||_2$ of the AENSZNN model (11) synthesized by the error function (5) converges to zero within a finite time.

Proof: The ith subsystem of the AENSZNN model (11) is written as $\dot{\delta}_i(t) = -G(\vec{\delta}(t))\delta_i(t) - \beta\int_0^t \delta_i(\tau)\mathrm{d}\tau$. For further investigation, the following Lyapnuov candidate function [32] is formulated:

$$l_i(t) = \delta_i^2(t) + (\beta(\int_0^t \delta_i(\tau)\mathrm{d}\tau)^2)/2 \geq 0. \tag{12}$$

Combining the equation (12) and $G(\cdot) > 0$, the following conclusions can be drawn:

$$G(\delta_i(t))\delta_i(t) = \begin{cases} > 0, & \delta_i(t) > 0 \text{ or } \delta_i(t) < 0, \\ = 0, & \delta_i(t) = 0, \end{cases} \tag{13}$$

which indicate that when $\delta_i(t) \neq 0$ or $\int_0^t \delta_i(\tau)\mathrm{d}\tau \neq 0$, the Lyapnuov candidate function $l_i(t) > 0$. If and only if $\delta_i(t) = \int_0^t \delta_i(\tau)\mathrm{d}\tau = 0$. Therefore, the Lyapunov function candidate $\delta_i(t)$ is positive definite. The derivative form of the function (12) can be expressed as

$$\begin{aligned} \dot{l}_i(t) = \frac{\mathrm{d}l_i(t)}{\mathrm{d}t} &= \delta_i(t)\dot{\delta}_i(t) + \beta\delta_i(t)\int_0^t \delta_i(\tau)\mathrm{d}\tau \\ &= \delta_i(t)(\dot{\delta}_i(t) + \beta\int_0^t \delta_i(\tau)\mathrm{d}\tau) \\ &= -G(\vec{\delta}(t))\delta_i^2(t) \leq 0. \end{aligned}$$

In other words, the $\dot{l}_i(t)$ is negative definite for all the time $t \in [0, +\infty)$. Thus, according to the Lyapunov theory, the residual error $||\vec{\delta}(t)||_2$ of the subsystem of the AENSZNN model (11) eventually converges to zero. It can be generalized and summarized that for each $i \in 1, 2, \ldots n$, the $\delta_i(t)$ globally converges to zero. Generally speaking, the error function $||\vec{\delta}(t)||_2$ globally converges to zero as time goes by. Thus, the proposed AENSZNN model (11) globally converges to the theoretical solution to the TVLEI problem (1) over finite time. The proof is thus completed. ■

IV. ROBUSTNESS ANALYSIS OF THE AENSZNN MODEL UNDER VARIOUS NOISES INFLUENCE

In practical application scenarios, the AENSZNN model (11) will unavoidably be influenced by various measurement noises, which will reduce the accuracy of the solving system or lead to the breakdown of the solving system. Therefore, considering the influence of measurement noises on the AENSZNN model (11) and further analyzing the various noises influence on the AENSZNN model (11), the formula of the AENSZNN model (11) interfered by measurement noises [33] is given as follows:

$$\begin{aligned} W(t)\dot{\vec{y}}(t) = &-\dot{W}(t)\vec{y}(t) + \dot{\vec{u}}(t) \\ &-G(\vec{\delta}(t))(W(t)\vec{y}(t) - \vec{u}(t)) \\ &-\beta\int_0^t (W(\tau)\vec{y}(\tau) - \vec{u}(\tau))\mathrm{d}\tau + \vec{\Phi}(t). \end{aligned} \tag{14}$$

The AENSZNN model (11) under the perturbations of constant noises, bounded random noises, and linear time-varying noises are provided severally. The following three theorems are given to analyze the robustness of the AENSZNN model (11).

Remark 1: Considering that solving continuou-time model directly is demanding. Therefore, the "ode45" differential equation solver in MATLAB is employed to convert the AENSZNN model (11) into an ordinary differential equation problem for simulation calculation. Specifically, the "ode45" differential equation solver uses the Runge-Kutta method to solve the target parameter $\vec{y}(t)$ in real time. After each iteration, the target parameter $\vec{y}(t)$ is substituted into the error function $\vec{\delta}(t)$ with the objective to compute the residual error $||\vec{\delta}(t)||_2$. The iteration stops when the residual error accuracy requirements are met.

Theorem 2: No matter how large amplitude of the constant noises $\vec{\Phi}(t) = \vec{\Phi} \in \mathbb{R}^{m+p}$ perturbed AENSZNN model (11), $\vec{\Phi}(t)$ can always globally converge to the theoretical solution of the TVLEI problem (1). Moreover, the ith subelement of $\vec{x}(t)$ in (11) globally converges to the theoretical solution of TVLEI problem (1).

Proof: By the definition of the Laplace transformation [34], the AENSZNN model (11) perturbed by constant noises $\vec{\Phi}(t) = \vec{\Phi} \in \mathbb{R}^{m+p}$ and $\Phi_i(t) = \Phi_i \in \mathbb{R}$ can be expressed as

$$s\delta_i(s) - \delta_i(0) = -G(\delta_i(s))\delta_i(s) - \frac{\beta}{s}\delta_i(s) + \frac{\bar{\Phi}_i}{s}, \tag{15}$$

According to the Laplace transformation [34] and the equation (15), we have:

$$\delta_i(s) = \frac{s(\delta_i(0) + \bar{\Phi}_i/s)}{s^2 + sG(\delta_i(s)) + \beta}. \tag{16}$$

As $t \to \infty$, $\lim_{t\to\infty} G(\delta_i(t)) = \lim_{s\to 0} G(\delta_i(s)) = \psi > 0$ is blue and the singularities of the transfer function $s/(s^2 + s\psi + \beta)$ are $s_1 = (-\psi + \sqrt{\psi^2 - 4\beta})/2$ and $s_2 = (-\psi - \sqrt{\psi^2 - 4\beta})/2$, respectively. In addition, the singularities of the transfer function is located on the left half of the plane due to $\psi > 0$ and $\beta > 0$. That is to say, the system satisfies the applicable condition of the Laplace final value theory [34]. Substituting the Laplace final value theory into equation (16):

$$\begin{aligned} \lim_{t\to\infty} \delta_i(t) &= \lim_{s\to 0} s\delta_i(s) = \lim_{s\to 0} \frac{s(\delta_i(0) + \bar{\Phi}_i/s)}{s^2 + G(\delta_i(s)) + \beta} \\ &= \lim_{s\to 0} \frac{s(\delta_i(0) + \bar{\Phi}_i/s)}{s^2 + s\psi + \beta} = 0. \end{aligned}$$

Obviously, the error function $\vec{\delta}(t)$ of the AENSZNN model (11) converges to zero. The proof is thus completed. ■

Theorem 3: The residual error $||\vec{\delta}(t)||_2$ of the proposed AENSZNN model (11) globally converges to a certain range under the interference term of the linear time-varying noises $\vec{\Phi}(t) = \Phi t \in \mathbb{R}^{m+p}$. Besides, $\Phi_i(t) = \Phi_i t \in \mathbb{R}$ represents the ith subelement of the $\vec{\Phi}(t)$. More precisely, $||\Phi||_2/\beta$ is the upper bound of the residual error $||\vec{\delta}(t)||_2$, it can successfully derive that when $\lim_{t\to\infty} ||\vec{\delta}(t)||_2 = 0$ as the parameter $\beta \to +\infty$.

Proof: On the basis of the definition of the Laplace transformation, the ith subelement of the mentioned AENSZNN model (11) can be written as

$$s\delta_i(s) - \delta_i(0) = -G(\delta_i(s))\delta_i(s) - \frac{\beta}{s}\delta_i(s) + \frac{\bar{\Phi}_i}{s^2}, \quad (17)$$

where the parameter $\bar{\Phi}_i/s^2$ represents the Laplace transformation of the linear time-varying noises $\bar{\Phi}_i t$ term. In terms of $\lim_{t\to\infty} G(\delta_i(t)) = \lim_{s\to 0} G(\delta_i(s)) = \psi > 0$. Therefore, equation (17) can be further summarized:

$$\delta_i(s) = \frac{s(\delta_i(0) + \bar{\Phi}_i/s^2)}{s^2 + s\psi + \beta}. \quad (18)$$

Taking the definition of Laplace final value theory and the Theorem 2 into account, we can obtain:

$$\begin{aligned}\lim_{t\to\infty} \delta_i(t) &= \lim_{s\to 0} s\delta_i(s) = \lim_{s\to 0} \frac{s(\delta_i(0) + \bar{\Phi}_i/s)}{s^2 + G(\delta_i(s)) + \beta} \\ &= \lim_{s\to 0} \frac{s(\delta_i(0) + \bar{\Phi}_i/s)}{s^2 + s\psi + \beta} \\ &= \frac{||\bar{\Phi}||_2}{\beta}.\end{aligned}$$

And we get that when the parameter $\beta \to +\infty$ for $\lim_{t\to\infty} ||\vec{\delta}(t)||_2 = 0$. The proof is completed. ■

When studying the AENSZNN model (11) for solving the TVLEI (1) problem with bounded random noises $\vec{\Phi}(t)$ perturbation and analyzing the robustness of the AENSZNN model (11), the following theorem is proposed.

Theorem 4: For the AENSZNN model (11) disturbed by bounded random noises $\vec{\Phi}(t) = \vec{\upsilon}(t) \in \mathbb{R}^{m+p}$, the upper bound of the steady-state residual error $|\vec{\delta}(t)||_2$ of the AENSZNN model (11) is $2\pi n/\sqrt{\psi^2 - 4\beta}$ when $\psi^2 > 4\beta$, the upper bound of the residual error $||\vec{\delta}(t)||_2$ is $4\psi\pi n/(\psi\sqrt{\psi^2 - 4\beta})$ for $\psi^2 < 4\beta$. Where the $\lim_{t\to\infty} G(\delta_i(t)) = \lim_{s\to 0} G(\delta_i(s)) = \psi > 0$. The parameter π expresses the $\max_{1\le i\le n^2}\{\max_{0\le\tau\le t}|\upsilon_i(\tau)|\}$ and the parameter $\upsilon_i(t)$ signifies the ith subelement of the random noises term $\vec{\upsilon}(t)$. That is to say, $\lim_{t\to\infty} ||\vec{\delta}(t)||_2$ is approximately inversely proportional to the adaptive scale factor $G(\cdot)$. It is worth noting that the maximum steady-state residual error converges to zero finally when the appropriate parameter is given and the adaptive scale factor $G(\cdot)$ is large enough.

Proof: Under the perturbation of bounded random noises $\vec{\upsilon}(t)$, the AENSZNN model (11) is expressed as

$$\dot{\vec{\delta}}(t) = -G(\vec{\delta}(t))\vec{\delta}(t) - \beta\int_0^t \vec{\delta}(\tau)\mathrm{d}\tau + \vec{\upsilon}(t),$$

where the ith subelement of $\dot{\vec{\delta}}(t)$ is

$$\dot{\delta}_i(t) = -G(\delta_i(t))\delta_i(t) - \beta\int_0^t \delta_i(\tau)\mathrm{d}\tau + \upsilon_i(t). \quad (19)$$

Thus, the upper steady-state residual error will be influenced by the values of ψ and β, where the parameter $\lim_{t\to\infty} G(\delta_i(t)) = \psi > 0$. For further decomposition and proof, let $\chi(t) = \int_0^t \vec{\delta}(\tau)\mathrm{d}\tau$ and $\chi_i(t) = \int_0^t \delta_i(\tau)\mathrm{d}\tau$. So when $t \to \infty$, equation (19) is rewritten as

$$\ddot{\chi}_i(t) + \psi\dot{\chi}_i(t) + \beta\chi_i(t) = \upsilon_i(t). \quad (20)$$

In addition, we define the parameters $\varepsilon_1 = (-\psi + \sqrt{\psi^2 - 4\beta})/2$ and $\varepsilon_2 = (-\psi + \sqrt{\psi^2 - 4\beta})/2$, and then discuss the proof in detail in the following three cases.

1) IN THE CASE OF $\psi^2 > 4\beta$

Based on the method for solving second-order differential equations, equation (19) can be converted into:

$$\begin{aligned}&\delta_i(t) \\ &= \frac{\delta_i(0)(\varepsilon_1\exp(\varepsilon_1 t) - \varepsilon_2\exp(\varepsilon_2 t))}{\varepsilon_1 - \varepsilon_2} \\ &\quad + \Big(\int_0^t (\varepsilon_1\exp(\varepsilon_1(t-\tau))) - \varepsilon_2\exp(\varepsilon_2(t-\tau)) \times \upsilon_i(\tau)\mathrm{d}\tau\Big) \\ &\quad \times \frac{1}{\varepsilon_1 - \varepsilon_2}.\end{aligned}$$

By the definition of the triangle inequality [35]:

$$\begin{aligned}|\delta_i(t)| &\le \frac{|\delta_i(0)(\varepsilon_1\exp(\varepsilon_1 t) - \varepsilon_2\exp(\varepsilon_2 t))|}{\varepsilon_1 - \varepsilon_2} \\ &\quad + \frac{2}{\varepsilon_1 - \varepsilon_2}\max|\upsilon_i(t)| \\ &= \frac{|\delta_i(0)(\varepsilon_1\exp(\varepsilon_1 t) - \varepsilon_2\exp(\varepsilon_2 t))|}{\varepsilon_1 - \varepsilon_2} \\ &\quad + \frac{2}{\sqrt{\psi^2 - 4\beta}}\max|\upsilon_i(t)|.\end{aligned}$$

In short, the following inequality can be obtained:

$$\lim_{t\to\infty} \sup||\vec{\delta}(t)||_2 \le \frac{2\pi n}{\sqrt{\psi^2 - 4\beta}}, \quad (21)$$

where $\sup(\cdot)$ represents the upper bound of the parameter.

2) IN THE CASE OF $\psi^2 = 4\beta$

Similar to the steps in $\psi^2 > 4\beta$, in this case, equation (19) can be written as

$$\begin{aligned}\delta_i(t) &= \delta_i(0)t\varepsilon_1\exp\varepsilon_1 t + \delta_i(0)\exp(\varepsilon_1 t) \\ &\quad + \int_0^t ((t-\tau)\varepsilon_1\exp(\varepsilon_1(t-\tau)))\upsilon_i(\tau)\mathrm{d}\tau \\ &\quad + \int_0^t \exp(\varepsilon_1(t-\tau))\upsilon_i(\tau)\mathrm{d}\tau. \quad (22)\end{aligned}$$

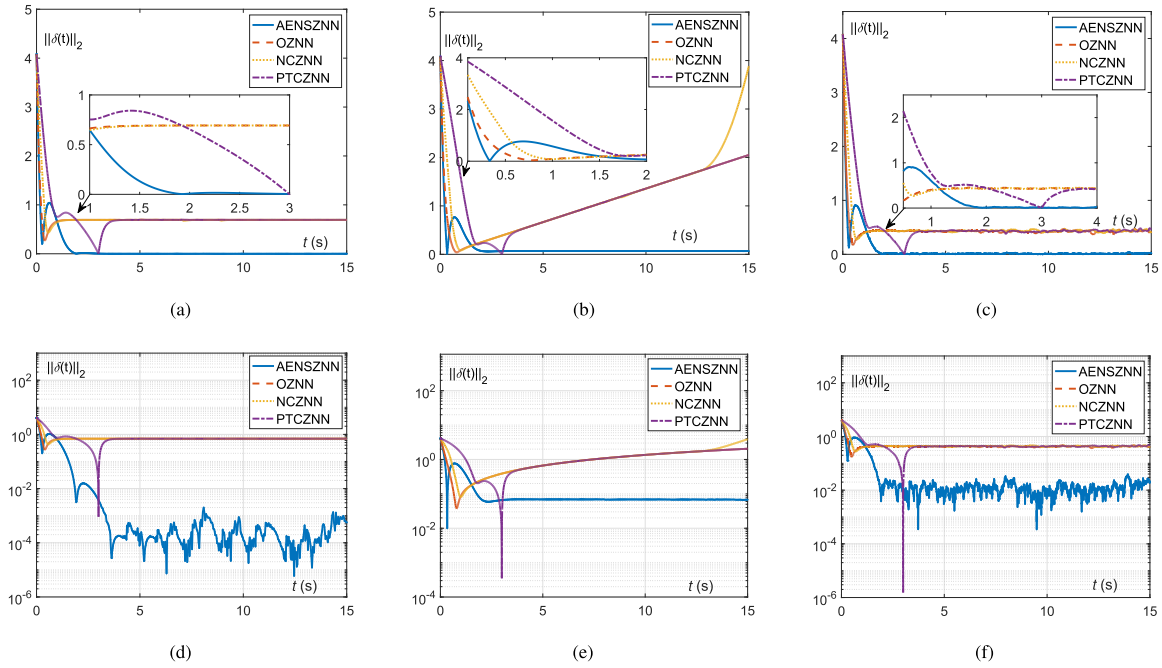

FIGURE 2. Property of the residual error $||\bar{\delta}(t)||_2$ comparing the OZNN model (7), NCZNN model (27), PTCZNN model (28), and the proposed AENSZNN model (11) with three kinds of measurement noises, where the initial value $\bar{x}(t) \in [-1, 1]^3$ is randomly generated. Making the initial value of the parameter of the proposed AENSZNN model (11) $G(t) = ||\bar{\delta}(t)||_2^2 + \mu$ and the other three models are $G(t) = ||\bar{\delta}(t)||_2^2 + 10$, $\beta = 10$ and $\gamma = 5$, respectively. (a) and (d) Show the residual error $||\bar{\delta}(t)||_2$ of models disturbed by bounded constant noises $\Phi(t) = \Phi = [2]^3$. (b) and (e) Depict the residual error $||\bar{\delta}(t)||_2$ of models propulted by linear time-varying noises $\Phi(t) = \bar{\Phi}t = [(2/5) \times t]^3$. (c) and (f) Denote the residual error $||\bar{\delta}(t)||_2$ of models propulted by bounded random noises $\Phi(t) \in [0.5, 2]^3$.

TABLE 3. Comparison results of OZNN model (7), NCZNN model (27), PTCZNN model (28), and the proposed AENSZNN model (11) in the three vital indicators: maximum steady state residual (MSSRE), average steady state residual (ASSRE), and convergent time to solve the TVLEI problem (1) when the parameters $G(t) = ||\bar{\delta}(t)||_2^2 + \beta$, $\beta = 10$ and $\gamma = 5$.

Model	ASSRE with NF	ASSRE with CN	ASSRE with TVN	ASSRE with RN	MSSRE with CN	MSSRE with TVN	MSSRE with RN
OZNN(7)	1.241×10^{-4}	6.376×10^{-1}	1.260×10^{0}	3.846×10^{-1}	6.696×10^{-1}	2.051×10^{0}	4.944×10^{-1}
NCZNN(27)	1.263×10^{-4}	6.159×10^{-1}	1.489×10^{0}	3.813×10^{-1}	6.963×10^{-1}	3.883×10^{0}	4.863×10^{-1}
PTCZNN(28)	1.703×10^{-4}	4.937×10^{-1}	1.164×10^{0}	2.490×10^{-1}	6.973×10^{-1}	2.051×10^{0}	4.758×10^{-1}
AENSZNN (11)	3.603×10^{-4}	1.593×10^{-4}	5.320×10^{-2}	8.500×10^{-3}	2.000×10^{-3}	6.930×10^{-2}	3.490×10^{-2}

⋆NF, CN, TVN, and RN signify the noises free, constant noises, linear time-varying noises, and bounded random noises, respectively.

It is worth noting that when $\psi^2 = 4\beta$ the parameter $\varepsilon_1 = -\psi/2$. Theorem 1 in paper [36] proves the existence of the constants $\omega > 0$ and $\iota > 0$ that satisfy the following inequality:

$$|\varepsilon_1| t \exp(\varepsilon_1 t) \leq \omega \exp(-\iota t). \tag{23}$$

And then, in combination with the definition of the triangle inequality and inequality (23), equation (22) can be transformed renewedly into:

$$\begin{aligned} |\delta_i(t)| \leq\ & |\delta_i(0)(\varepsilon_1 \exp(\varepsilon_1 t) - \varepsilon_2 \exp(\varepsilon_2 t))| \\ & + \int_0^t |\omega \exp(-\iota(t-\tau))||\upsilon_i(t)| \mathrm{d}\tau \\ & + \int_0^t |\exp(\varepsilon_1(t-\tau))||\upsilon_i(t)| \mathrm{d}\tau. \end{aligned}$$

The above inequality is simplified and rearanged to obtain:

$$|\delta_i(t)| \leq |\delta_i(0)(\varepsilon_1 \exp(\varepsilon_1 t) - \varepsilon_2 \exp(\varepsilon_2 t))| + (\frac{\omega}{\iota} - \frac{1}{\varepsilon_1})\pi.$$

On the basis of the above facts we can reach the following conclusion:

$$\lim_{t \to \infty} \sup ||\vec{\delta}(t)||_2 \leq (\frac{\omega}{\iota} - \frac{1}{\varepsilon_1})\pi n. \tag{24}$$

3) IN THE CASE OF $\psi^2 < 4\beta$

Similar to the previous case of $\psi^2 > 4\beta$ and $\psi^2 = 4\beta$, when $\psi^2 < 4\beta$, the following equation is satisfied:

$$\lim_{t \to \infty} \sup ||\vec{\delta}(t)||_2 \leq \frac{2\pi\beta n}{\psi\sqrt{4\beta - \psi^2}}. \tag{25}$$

It can draw a conclusion that the proposed AENSZNN model (11) not only uses a competitive adaption scale factor to increase the convergence speed of the model, but also maintains excellent robustness under various noises disturbance by using the momentum information. Moreover, it is possible to solve the TVLEI problem (1) without being affected by the lagging error due to the consideration of the

AENSZNN model (11) which utilizes the derivative term of the system. The proof is thus completed. ■

V. SIMULATION EXPERIMENTS AND COMPARISONS

In this section, the effectiveness and superiority of the proposed AENSZNN model (11) for the solving TVLEI problem (1) are proved through comparative numerical experiments. The simulations are carried out on a digital computer with Intel Core i7-8565U @1.80 GHz CPU, 16 GB memory, and Windows 10 operating system using MATLAB R2016b.

A. EXAMPLE 1

Based on formula (1), take the following time-varying matrices and vectors as a typical example of simulation experiments:

$$C(t) = \begin{bmatrix} \sin(t)+2 \\ \cos(t)+3 \\ -\sin(t)+4 \end{bmatrix}^{\mathrm{T}}, \quad \vec{b}(t) = \begin{bmatrix} \sin(2t)+\cos(2t) \end{bmatrix}$$

$$D(t) = \begin{bmatrix} \sin(3t) & -\cos(3t) \\ \cos(3t) & \sin(3t) \\ -\sin(3t) & \cos(3t) \end{bmatrix}^{\mathrm{T}}, \quad \vec{d}(t) = \begin{bmatrix} \sin(4t) \\ \cos(4t) \end{bmatrix}.$$

The adaptive scale factor G(·) and parameter γ of the proposed AENSZNN model (11) are set as $G(t) = ||\vec{\delta}(t)||_2^2 + 10$, $\beta = 10$ and $\gamma = 5$. On the basis of the above theoretical analysis, such a TVLEI problem (1) can be transformed into a time-varying matrix-vector equation (2). The corresponding simulation results are shown in Figs. 2 and 4. Among them, when solving example 1 (V-A), the residual error $||\vec{\delta}(t)||_2$ of the AENSZNN model (11) globally converges from the initial state to the theoretical solution. In addition, the following models are utilized to solve the TVLEI problem (1) and their specific evolution formula are as follows:

- OZNN model.

$$W(t)\dot{\vec{y}}(t) = -\dot{W}(t)\vec{y}(t) - \gamma(W(t)\vec{y}(t) - \vec{u}(t)) + \dot{\vec{u}}(t). \tag{26}$$

- NCZNN model in [20].

$$W(t)\dot{\vec{y}}(t) = -\dot{W}(t)\vec{y}(t) - \gamma\Theta(W(t)\vec{y}(t) - \vec{u}(t)) + \dot{\vec{u}}(t), \tag{27}$$

where the $\Theta(\cdot)$ denotes the non-convex and bounded activation function.

- PTCZNN model in [29].

$$W(t)\dot{\vec{y}}(t) = -\dot{W}(t)\vec{y}(t) + \dot{\vec{u}}(t) - \gamma\Upsilon(W(t)\vec{y}(t) - \vec{u}(t)), \tag{28}$$

where the $\Upsilon(\cdot)$ represents the odd monotonically increasing activation function arrary.

B. NOISES FREE CONDITION

Specifically, Fig. 4 illustrates the simulation results of Example 1 (V-A) solved by the AENSZNN model (11) with noises free condition. In addition, it is worth stating briefly in advance that maximal steady-state residual error (MSSRE) is defined as $\lim_{t\to\infty}\sup||\vec{\delta}(t_m)||_2, t_m \in [t_s, t_{\max}]$ and average steady-state residual error (ASSRE) is calculatated by $\int_{t_s}^{t_{\max}} ||\vec{\delta}(\tau)||_2 \mathrm{d}\tau/(t_{\max} - t_s)$. There are thirty random initial states are set at the beginning of the experiment, and the simulation results synthesized by the AENSZNN model (11) based on the norm adaptive factor $G(\cdot)$ gradually approached the theoretical solution of the problem, the trajectory shape of the simulation result is exhibited in Fig. 4 (a) and (d). Among them, when solving example 1 (V-A), the AENSZNN model (11) globally converges from the initial state to the theoretical solution. What needs to be explained here is that the $t(s)$ in all figures represents the length of time in seconds. From the Fig. 4 (b), it shows that the order of the residual $||\vec{\delta}(t)||_2$ (11) generated by the AENSZNN model is 10^{-6}, while other models converge to 10^{-4}. Therefore, compared with the OZNN model (7), NCZNN model (27), and PTCZNN model (28), the AENSZNN model (11) proposed in dealing with the TVLEI problem (1) achieves higher computational accuracy. It is worth mentioning that because the AENSZNN model (11) integrates the norm-based adaption factor $G(\cdot)$, the expected experimental results can be obtained without repeated adjustment of the convergence coefficient.

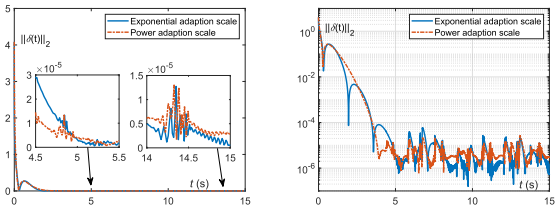

(a) (b)

FIGURE 3. The convergence performance of the AENSZNN model (11) with adaptive scale parameter (9) and (10), respectively. (a) Represents the residual error $||\vec{\delta}(t)||_2$. (b) Denotes the logarithmic residual error $||\vec{\delta}(t)||_2$.

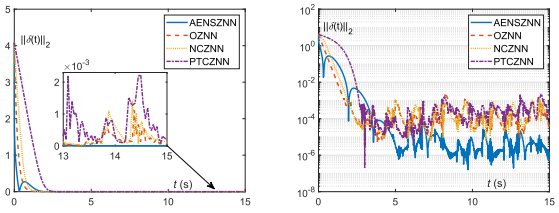

(a) (b)

FIGURE 4. Residual error $||\vec{\delta}(t)||_2$ of the OZNN model (7), NCZNN model (27), PTCZNN model (28), and the AENSZNN model (11). (a) Represents the residual error $||\vec{\delta}(t)||_2$. (b) Denotes the logarithmic residual error $||\vec{\delta}(t)||_2$.

C. NOISES CONDITION

Fig. 2 (a) and (b) illustrate the simulation results of the OZNN model (7), NCZNN model (27), and PTCZNN model (28) used to solve the TVLEI problem (1) in the case of the constant noises. In order to study and verify the global convergence and robustness of the AENSZNN model (11)

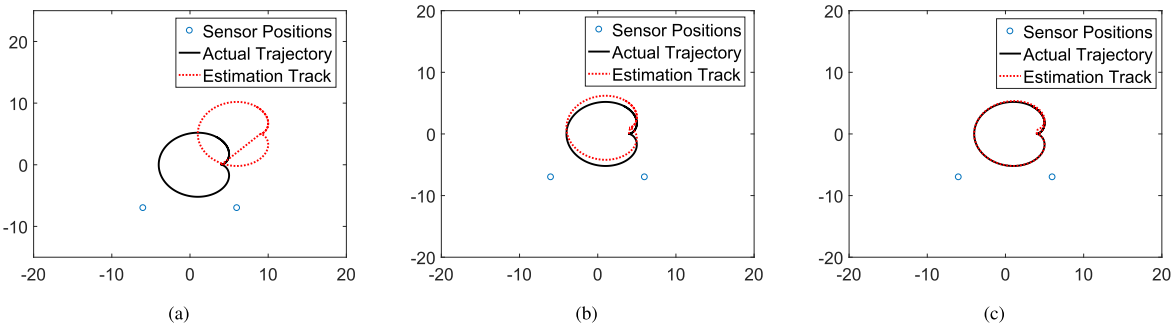

FIGURE 5. The comparative experimental results of the Pseudo-inverse method, OZNN model (7), and the proposed AENSZNN model (11) to solve the dynamic 2-D positioning problem. Among them, (a)–(c) Display the actual trajectory of the pseudo-inverse method, OZNN model (7), and AENSZNN model (11) and the resulting estimation trace fitting diagrams one by one.

TABLE 4. AOA algorithm arithmetic form meaning.

Arithmetic form	practical significance
$\vec{y}(t) = [x(t); y(t)]$	the target position at time t
(x_i, y_i)	the coordinates of the sensor node
$Q = \begin{bmatrix} x_1 & x_2 & \cdots & x_n \\ y_1 & y_2 & \cdots & y_n \end{bmatrix}$	the coordinate matrix of n sensor nodes
$\vec{\alpha}_i(t)$	the incident angle of the sensor node

in the case of constant noises, set the constant noises to $\Phi(t) = \Phi = [2]^3$, and proceed with corresponding numerical simulation experiments are carried out. Specifically, the residual error $||\vec{\delta}(t)||_2$ of the AENSZNN model (11) proposed in this paper converges to 10^{-3} within 2s in the disturbance environment of constant noises. By comparison, the residual errors of the OZNN model (7), NCZNN model (27), and PTCZNN model (28) are still at the value of 1 with the parameter $\gamma = 5$.

For the sake of the robustness of the AENSZNN model (11) can be further studied under the disturbance of linear time-varying noises $\Phi(t) = \bar{\Phi}t = [(2/5) \times t]^3$ and bounded random noises $\Phi(t) \in [0.5, 2]^3$. As can be seen from Fig. 2 (c)–(f) that the residual error $||\vec{\delta}(t)||_2$ of the AENSZNN model (11) converges to of order 10^{-1} and of order 10^{-2} under the disturbance of linear noises and bounded random noises. In other words, even if the AENSZNN model (11) is interfered with by linear time-varying noises and bounded random noises, it still maintains high accuracy. At the same time, it can be seen that the residual error $||\vec{\delta}(t)||_2$ obtained from the OZNN model (7), NCZNN model (27), and PTCZNN model (28) are relatively large. Therefore, when solving Example 1 (V-A) by the AENSZNN model (11) that uses norm-based adaption coefficient to regulate the convergence coefficient, the AENSZNN model (11) still maintains strong robustness despite constant noises disturbance.

D. AOA ALGORITHM

The angle of arrival (AOA) [37] dynamic positioning algorithm is a positioning scheme that relies on the angle of arrival between the measurement target and the sensor node. Specifically, the intersection of two rays passing through the target with the sensor node as the starting point is the site of the target. Moreover, Table 4 shows the arithmetic notations of the following problem descriptions.

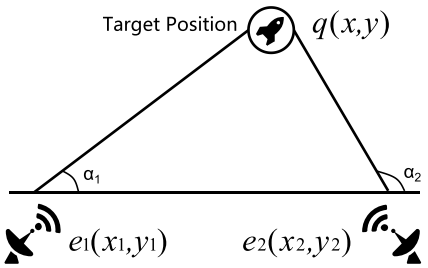

FIGURE 6. Outline map based on AOA dynamic positioning programme.

The AOA dynamic positioning algorithm is a positioning scheme that relies on the angle of arrival between the measurement target and the sensor node. Specifically, as shown in the schematic diagram of Fig. 6, the intersection of the two rays $e_1(x_1, y_1)$ and $e_2(x_2, y_2)$ passing through the target with the sensor node as the starting point is the position $q(x, y)$ where the dynamic target is located. In addition, for the convenience of notation and description, the Table 4 shows the arithmetic symbols described in the following problem.

For the convenience of research, the incident angle can be expressed as

$$\tan(\alpha_i(t)) = \frac{y(t) - y_i}{x(t) - x_i}.$$

By further derivating, the following equation can be obtained

$$\begin{bmatrix} y_1 - x_1(t)\tan\alpha_1 \\ y_2 - x_2(t)\tan\alpha_2 \\ \vdots \\ y_n - x_n(t)\tan\alpha_n \end{bmatrix} = \begin{bmatrix} -\tan\alpha_1 & 1 \\ -\tan\alpha_2 & 1 \\ \vdots & \\ -\tan\alpha_n & 1 \end{bmatrix} \begin{bmatrix} x(t) \\ y(t) \end{bmatrix}. \tag{29}$$

For further discussion, the equation (29) is expressed in the following form:

$$Q(t)\vec{e}(t) = \vec{a}(t), \tag{30}$$

where the $Q(t) \in \mathbb{R}^{n\times 2}$, $\vec{e}(t) = [x(t), y(t)]^{\mathrm{T}}$ and $\vec{a}(t) \in \mathbb{R}^n$.

Moreover, to more intuitively observe the superiority of the proposed AENSZNN model (11) compared to different models, the visual simulation results of the AENSZNN model (11) and the OZNN model (7) while calculating the

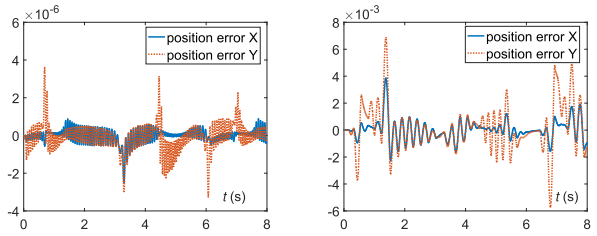

(a) (b)

FIGURE 7. (a) and (b) Manifest the 2-D position errors compounded by the OZNN model (7), and proposed AENSZNN model (11) severally.

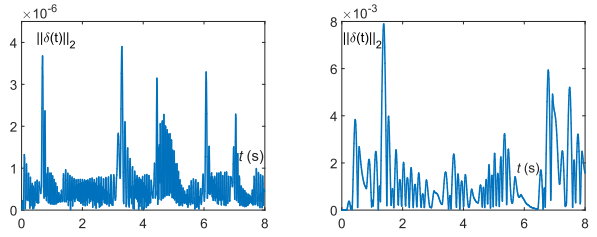

(a) (b)

FIGURE 8. Comparison between OZNN model (7) and AENSZNN model (11) in the application of 2-D dynamic positioning estimation. (a) Tracking residual error $||\vec{\delta}(t)||_2$ of AENSZNN model (11), (b) Tracking residual error $||\vec{\delta}(t)||_2$ of OZNN model (7).

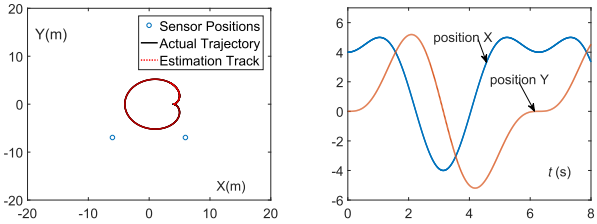

(a) (b)

FIGURE 9. Verification results of the AENSZNN model (11) in the application of dynamic mobile target localization estimation. (a) The actual trajectory and estimated trajectory fitting result of the mobile positioning target synthesized by the AENSZNN model (11), (b) The 2-D positioning error generated by the AENSZNN model (11).

pseudoinverse of $W(t)$ are shown in Fig. 8. It can be obviously seen that compared with the OZNN model (7), the proposed AENSZNN model (11) achieves better robust performance and obtains higher solution accuracy. Furthermore, in order to more intuitively observe the superiority of the proposed AENSZNN model (11) relative to different models, the AENSZNN model (11) is compared with the classic OZNN model (7) and the pseudo-inverse iterative solution method for solving the time-varying problems while calculating the pseudoinverse of $W(t)$. Fig. 5 (a)–(c) respectively show the actual trajectory and estimation trace fitting diagrams and steady-state residual error $||\vec{\delta}(t)||_2$ convergent curves obtained by using the pseudo-inverse method, the OZNN model (7), and the AENSZNN model (11) proposed in this article as several solutions for solving two-dimensional dynamic positioning problem. It can be obviously seen that compared with the OZNN model (7) and the pseudo-inverse solution method, the proposed AENSZNN model (11) achieves a better robust performance and obtains a higher solution accuracy in Fig. 8. Carefully observe the comparison result image, it is obvious that when the constant noises $\vartheta(t)$ is set as 5, the estimation trajectory obtained by the pseudo-inverse method deviates from the actual trajectory to a large extent; the forecast result of the OZNN model (7) deviates from the actual trajectory to a small extent. However, the AENSZNN model (11) can still obtain almost the same estimation trajectory results as the actual trajectory even under the interference of noises, and steady-state residual error $||\vec{\delta}(t)||_2$ can converge faster.

VI. CONCLUSION AND FUTURE WORK

In this paper, we propose an adaptive enhanced and noise-suppressing zeroing neural network termed the AENSZNN model for solving the TVLEI problem (1) in the field of practical engineering. Furthermore, to study and confirm the reliability of applying the adaption scale factor to the ZNN model for the first time, the residual error $||\vec{\delta}(t)||_2$ of exponential adaption scale factor (9) and power adaption scale factor (10) is shown in Fig. 3 (a) and (b). Specifically, the AENSZNN model adopts exponential adaption scale factor (9) and power adaption scale factor (10) accurately converge to 10^{-6}, within 5 seconds. As a follow-up to this article, we will further optimize the adaptive scale factor to improve the convergence and robustness of the AENSZNN model. Besides, we will explore and give rein to the superiority of the AENSZNN model in response to TVLEI problem encountered in other practical application scenarios.

REFERENCES

[1] C. Hua and Y. Wang, "Delay-dependent stability for load frequency control system via linear operator inequality," *IEEE Trans. Cybern.*, early access, Dec. 11, 2021, doi: 10.1109/TCYB.2020.3037113.
[2] J. C. Arceo, M. Sánches, V. Estrada-Manzo, and M. Bernal, "Convex stability analysis of nonlinear singular systems via linear matrix inequalities," *IEEE Trans. Autom. Control*, vol. 64, no. 4, pp. 1740–1745, Apr. 2019.
[3] Q. Ding, G. Weng, G. Zhao, and C. Hu, "Efficient and secure outsourcing of large-scale linear system of equations," *IEEE Trans. Cloud Comput.*, vol. 9, no. 2, pp. 587–597, Apr. 2021.
[4] M. A. Anam, I. Anarado, and Y. Andreopoulos, "Generalized numerical entanglement for reliable linear, sesquilinear and bijective operations on integer data streams," *IEEE Trans. Emerg. Topics Comput.*, vol. 6, no. 4, pp. 474–487, Oct. 2018.
[5] Q. Zhu and M. L. Shyu, "Sparse linear integration of content and context modalities for semantic concept retrieval," *IEEE Trans. Emerg. Topics Comput.*, vol. 3, no. 2, pp. 152–160, Jun. 2015.
[6] Y. Xia, G. Feng, and J. Wang, "A primal-dual neural network for online resolving constrained kinematic redundancy in robot motion control," *IEEE Trans. Syst., Man, Cybern., B, Cybern.*, vol. 35, no. 1, pp. 54–64, Feb. 2005.
[7] J. Dai, Y. Li, L. Xiao, L. Jia, Q. Liao, and J. Li, "Comprehensive study on complex-valued ZNN models activated by novel nonlinear functions for dynamic complex linear equations," *Inf. Sci.*, vol. 561, pp. 101–114, Jun. 2021.
[8] M. C. Valentino, F. A. Faria, V. A. Oliveira, and L. F. C. Alberto, "Sufficient conditions in terms of linear matrix inequalities for guaranteed ultimately boundedness of solutions of switched Takagi–Sugeno fuzzy systems using the S-procedure," *Inf. Sci.*, vol. 572, pp. 501–521, Sep. 2021.
[9] X. Yi, X. Li, L. Xie, and K. H. Johansson, "Distributed online convex optimization with time-varying coupled inequality constraints," *IEEE Trans. Signal Process.*, vol. 68, pp. 731–746, 2020.

[10] G. Wang, X. Cai, Z. Cui, G. Min, and J. Chen, "High performance computing for cyber physical social systems by using evolutionary multi-objective optimization algorithm," *IEEE Trans. Emerg. Topics Comput.*, vol. 8, no. 1, pp. 20–30, Jan./Mar. 2020.
[11] L.-P. Pang, E. Spedicato, Z.-Q. Xia, and W. Wang, "A method for solving the system of linear equations and linear inequalities," *Math. Comput. Model.*, vol. 46, nos. 5–6, pp. 823–836, 2007.
[12] E. Castillo, A. J. Conejo, R. E. Pruneda, and C. Solares, "Observability in linear systems of equations and inequalities: Applications," *Comput. Oper. Res.*, vol. 34, no. 6, pp. 1708–1720, 2007.
[13] C. Jiang, L. Jin, and X. Xiao, "Residual-based adaptive coefficient and noise-immunity ZNN for perturbed time-dependent quadratic minimization," 2021, *arXiv:2112.01773*.
[14] A. I. Golikov and Y. G. Evtushenko, "Regularization and normal solutions of systems of linear equations and inequalities," *Proc. Steklov Inst. Math.*, vol. 289, no. 1, pp. 102–110, 2015.
[15] H. Li, J. Luo, and Q. Wang, "Solvability and feasibility of interval linear equations and inequalities," *Linear Algebra Appl.*, vol. 463, pp. 78–94, Dec. 2014.
[16] Z. Zhongcheng, "Lyapunov inequality for linear elliptic equation, an optimal control approach," in *Proc. 27th Chin. Control Conf.*, Jul. 2008, pp. 610–613.
[17] Y. Xia, J. Wang, and D. L. Hung, "Recurrent neural networks for solving linear inequalities and equations," *IEEE Trans. Circuits Syst. I, Fundam. Theory Appl.*, vol. 46, no. 4, pp. 452–462, Apr. 1999.
[18] X.-B. Liang and S. K. Tso, "Improved upper bound on step-size parameters of discrete-time recurrent neural networks for linear inequality and equation system," *IEEE Trans. Circuits Syst. I, Fundam. Theory Appl.*, vol. 49, no. 5, pp. 695–698, May 2002.
[19] Z. Hu, K. Li, K. Li, J. Li, and L. Xiao, "Zeroing neural network with comprehensive performance and its applications to time-varying Lyapunov equation and perturbed robotic tracking," *Neurocomputing*, vol. 418, pp. 79–90, Dec. 2020.
[20] C. Jiang, X. Xiao, D. Liu, H. Huang, H. Xiao, and H. Lu, "Non-convex and bound constraint zeroing neural network for solving time-varying complex-valued quadratic programming problem," *IEEE Trans. Ind. Informat.*, vol. 17, no. 10, pp. 6864–6874, Oct. 2021, doi: 10.1109/TII.2020.3047959.
[21] Y. Zeng, L. Xiao, K. Li, J. Li, K. Li, and Z. Jian, "Design and analysis of three nonlinearly activated ZNN models for solving time-varying linear matrix inequalities in finite time," *Neurocomputing*, vol. 390, pp. 78–87, May 2020.
[22] X. Xiao, C. Jiang, H. Lu, L. Jin, D. Liu, H. Huang, and Y. Pan, "A parallel computing method based on zeroing neural networks for time-varying complex-valued matrix Moore–Penrose inversion," *Inf. Sci.*, vol. 524, pp. 216–228, Jul. 2020.
[23] F. Xu, Z. Li, Z. Nie, H. Shao, and D. Guo, "Zeroing neural network for solving time-varying linear equation and inequality systems," *IEEE Trans. Neural Netw. Learn. Syst.*, vol. 30, no. 8, pp. 2346–2357, Aug. 2019.
[24] J. Zhang, L. Jin, and L. Cheng, "RNN for perturbed manipulability optimization of manipulators based on a distributed scheme: A game-theoretic perspective," *IEEE Trans. Neural Netw. Learn. Syst.*, vol. 31, no. 12, pp. 5116–5126, Dec. 2020.
[25] X. Zhang, L. Wu, and S. Cui, "An improved integral inequality to stability analysis of genetic regulatory networks with interval time-varying delays," *IEEE/ACM Trans. Comput. Biol. Bioinformat.*, vol. 12, no. 2, pp. 398–409, Feb. 2015.
[26] T. Yu, J. Liu, Q. Zeng, and L. Wu, "Dissipativity-based filtering for switched genetic regulatory networks with stochastic disturbances and time-varying delays," *IEEE/ACM Trans. Comput. Biol. Bioinf.*, vol. 18, no. 3, pp. 1082–1092, May 2021.
[27] L. Jin, S. Li, B. Hu, M. Liu, and J. Yu, "A noise-suppressing neural algorithm for solving the time-varying system of linear equations: A control-based approach," *IEEE Trans. Ind. Informat.*, vol. 15, no. 1, pp. 236–246, Jan. 2019.
[28] L. Xiao, K. Li, and M. Duan, "Computing time-varying quadratic optimization with finite-time convergence and noise tolerance: A unified framework for zeroing neural network," *IEEE Trans. Neural Netw. Learn. Syst.*, vol. 30, no. 11, pp. 3360–3369, Nov. 2019.
[29] Z. Hu, L. Xiao, J. Dai, Y. Xu, Q. Zuo, and C. Liu, "A unified predefined-time convergent and robust ZNN model for constrained quadratic programming," *IEEE Trans. Ind. Informat.*, vol. 17, no. 3, pp. 1998–2010, Mar. 2021.
[30] L. Xiao, B. Liao, S. Li, Z. Zhang, L. Ding, and L. Jin, "Design and analysis of FTZNN applied to the real-time solution of a nonstationary Lyapunov equation and tracking control of a wheeled mobile manipulator," *IEEE Trans. Ind. Informat.*, vol. 14, no. 1, pp. 98–105, Jan. 2018.
[31] K. Li, Y. Pan, and S. Q. Zheng, "Fast and processor efficient parallel matrix multiplication algorithms on a linear array with a reconfigurable pipelined bus system," *IEEE Trans. Parallel Distrib. Syst.*, vol. 9, no. 8, pp. 705–720, Aug. 1998.
[32] S.-Y. Li, C.-H. Yang, S.-A. Chen, L.-W. Ko, and C.-T. Lin, "Fuzzy adaptive synchronization of time-reversed chaotic systems via a new adaptive control strategy," *Inf. Sci.*, vol. 222, pp. 486–500, Feb. 2013.
[33] A. Khodamoradi and R. Kastner, "$O(N)$-space spatiotemporal filter for reducing noise in neuromorphic vision sensors," *IEEE Trans. Emerg. Topics Comput.*, vol. 9, no. 1, pp. 15–23, Jan./Mar. 2021.
[34] A. V. Oppenheim and A. S. Willsky, *Signals and Systems*. Englewood Cliffs, NJ, USA: Prentice-Hall, 1997.
[35] L. Jin, Y. Zhang, S. Li, and Y. Zhang, "Modified ZNN for time-varying quadratic programming with inherent tolerance to noises and its application to kinematic redundancy resolution of robot manipulators," *IEEE Trans. Ind. Electron.*, vol. 63, no. 11, pp. 6978–6988, Nov. 2016.
[36] Z. Zhang and Y. Zhang, "Design and experimentation of acceleration-level drift-free scheme aided by two recurrent neural networks," *IET Control Theory Appl.*, vol. 7, no. 1, pp. 25–42, Jan. 2013.
[37] G. Han, X. Yang, L. Liu, W. Zhang, and M. Guizani, "A disaster management-oriented path planning for mobile anchor node-based localization in wireless sensor networks," *IEEE Trans. Emerg. Topics Comput.*, vol. 8, no. 1, pp. 115–125, Jan. 2020.

CHAOMIN WU is currently pursuing the B.S. degree in automation with Guangdong Ocean University, Guangdong, China. Her research interests include intelligent algorithms, computer vision, and neural networks.

ZIFAN HUANG is currently pursuing the B.S. degree in automation with Guangdong Ocean University, Guangdong, China. Her research interests include intelligent algorithms, image processing, and deep learning.

JIAHAO WU received the B.E. degree in communication engineering from Guangdong Ocean University, Zhanjiang, China, in 2020, where he is currently pursuing the M.Agr. degree in agricultural engineering and information technology with the School of Electronics and Information Engineering. His current research interests include neural networks and computer vision.

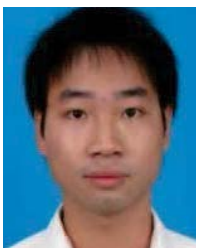

CONG LIN received the B.S. and M.S. degrees from the Guangxi University of Science and Technology, China, in 2011 and 2015, respectively. He is currently pursuing the Ph.D. degree with Hainan University, China. He is currently a Lecturer with the School of Information and Communication Engineering, Guangdong Ocean University. His current research interests include machine learning and image processing.